Towards High Fidelity High Efficiency MEMS Microspeakers

I. Shahosseini, E. Lefeuvre, M. Woytasik, J. Moulin, X. Leroux, S. Edmond, E. Dufour-Gergam, A. Bosseboeuf
Institut d'Electronique Fondamentale, Univ. Paris Sud
Bat. 220, 91405 Orsay, France
iman.shahosseini@u-psud.fr

G. Lemarquand, V. Lemarquand
Laboratoire d'Acoustique de l'Université du Maine
Avenue Olivier Messiaen, 72085 Le Mans, France

***Abstract*— This paper presents simulations and microfabrication of different parts of high fidelity electrodynamic MEMS loudspeakers with high electroacoustic conversion efficiency. The originality of the structure lies on the use of rigid silicon membranes suspended by a whole set of silicon beams instead of flexible polymer membranes usually found in MEMS loudspeakers. The microspeaker structure includes a planar copper microcoil electroplated on the silicon membrane and permanent magnets bonded on the substrate. Microstructure of the silicon membrane was optimized using FEM simulations for providing both rigidity and lightness of the mobile part. The results presented on a deep RIE etched 15 mm diameter silicon membrane structured with 40 stiffening ribs and on a 30 µm thick microcoil with 35 turns experimentally show the feasibility of key stages required for manufacturing of MEMS microspeakers with outstanding properties.**

I. INTRODUCTION

Industrial demand for microspeakers with higher power and better quality is strongly increasing with the broad development of various mobile devices. Furthermore, autonomy of mobile devices is a critical issue, so another important goal is reducing the consumption. Taking the example of cellular phones, up to one quarter of total consumption in free hand mode is due to the audio system. To give an example of how important this problem is for industry, it is enough to mention that more than one billion cell phones have been sold all over the world just in year 2009. Microspeakers used in mobile devices have, moreover, very poor sound quality compared to that of conventional loudspeakers. All these facts show that conventional processes used until now for manufacturing so called microspeakers are reaching their limits in terms of integration, efficiency, and sound quality. At this point, microsystems technology (MST) reveals new horizons to overcome such limitations. MST not only does decrease the fabrication costs, thanks to the batch processing, but also it yields good reproducibility and good dimensional precision.

As Table I presents, the drive force of such MST microspeakers stems from various actuation mechanisms. Among them these types can be highlighted: piezoelectric, electrostatic, and electrodynamic. Besides, they exist loudspeakers which are based on electrostrictive effect of polymer films or thermo-acoustic properties of carbon nanotubes. For our work, neither piezoelectric actuation is satisfying because of nonlinearities, nor electrostatic actuations because of its need for high driving voltage. As shown by recent studies, electrodynamics actuation principle is the best way to meet the objective requirements: producing high sound pressure level (SPL), having a linear response, and getting a high fidelity sound reproduction. In this kind of actuator the driving force, the Lorentz force, is resulted from the interaction between inductive coil driven by the electrical current and radical component of magnetic field observed by the coil [1]:

$$F_{Lorentz} = \sum_{i=1}^{N} I.2\pi.R_i.B_r(R_i) \qquad (1)$$

where I is the coil current, R_i the radius of each turn, and B_r the radial component of magnetic field in the coil plane.

Our work is presented in five sections. The next part of this paper unveils a new design of an electrodynamics MEMS microspeaker. In the third part, analytical models determine dimensions of different components of the device, and with the help of finite element method (FEM) the design is optimized both in terms of efficiency and acoustic performance. Then, after presenting technological steps and microfabrication results, the future work is outlined.

II. DEVICE DESIGN

Instead of deformable diaphragms used in most of the MEMS microspeakers to generate acoustic waves [1-8,10], a stiff and light membrane is employed here. Usually, deformable diaphragm, such as parylene or polyimide, is clamped to the substrate on out side edge, so the principal vib-

This work is sponsored by French Agence Nationale pour la Recherche

TABLE I. SUMMARY TABLE OF DIFFERENT WORKS

Actuation Type	Manufacturer	Material for membrane	Membrane size	Maximum SPL	Frequency	Measurement distance
Piezoelectric	S. H. Yi and E. S. Kim [2]	ZnO	5 mm x 5 mm	92 dB	3 kHz	0.2 cm
	H. C. Cho et al [3]	AlN	-	100 dB	9.3 kHz	1 cm
	S. C. Ko et al [4]	ZnO	3 mm x 3 mm x 3 µm	83,1 dB	13.3 kHz	1 cm
	S. S. Lee and R. M. White [5]	ZnO	2 mm x 2 mm x 4.7 µm	70 dB	5 kHz	0.5 cm
Electrostatic	P. Rangsten et al [6]	Silicon	2 mm*	112 dB	127 kHz	1 cm
	R. C. Roberts et al [7]	Poly-SiC	0.8 mm*	73 dB	16.6 kHz	1 cm
Electrostrictive	R. Heydt et al [8]	Silicon rubber	-	100 dB	> 1.5 kHz	100 cm
Thermoacoustic	L. Xiao et al [9]	Carbon Nanotubes	30 mm x 30 mm (one layer)	85 dB	10 kHz	5 cm
			30 mm x 30 mm (four layers)	95 dB	10 kHz	5 cm
Electrodynamic	M. C. Cheng et al [10]	Polyimide	3.5 mm*	93 dB	5 kHz	2 cm^3 chamber
	Je et Chae [1]	Polyimide	3 mm*	106 dB	1 kHz	1.3 cm
	This work	**Silicon**	**15 mm***	**70 dB****	**0.3 kHz****	**10 cm****

* Membrane diameter ** Objective values of this work

ration mode of such microspeaker is drum mode. However, while using a rigid membrane held by low stiffness suspension beams, as depicted in Fig. 1, the fundamental vibration mode is piston mode; which means entire surface of the membrane runs in parallel to the original position. Acoustically speaking, this is the best way to get high quality sound reproduction. Moreover, for the same surface of diaphragm and for the same displacement, the volume of the displaced air is bigger than with the other structures, so higher SPL can be obtained.

As shown in Fig. 1, planar coil is located on top of the membrane. And to feed it, two conductor tracks are put on the suspension beams. To prevent the coil from short circuits, an electrically insulator layer with two vias comes between the coil and the conductor tracks. These elements with the membrane define the mobile part of the microspeaker. Two magnet rings are located on the front and back sides of the substrate all around the coil to induce maximum of radial magnetic field. An inset of microstructured membrane backside, which is studied in the next part, is also shown in this figure.

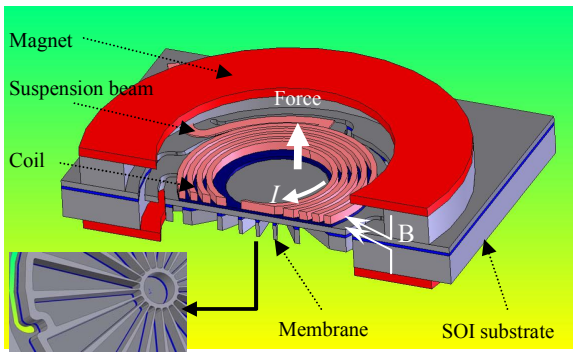

Figure 1. : Cut view of the microspeaker and bottom view of the membrane

As stated, it is important for sound quality to have on one hand a rigid membrane which resists undesirable deformations, and on the other hand a light membrane to keep the efficiency as high as possible, as it will be detailed in the next section. Thus, a high ratio of Young's modulus to density is needed. Table II shows that Si and Al_20_3 have relatively high ratio compared to other materials. As large panel of micromachining processes are optimized for Si, it is selected for the membrane and its mechanical properties are taken for further calculations.

III. DEVICE DIMENSIONNING

A. *Analytical analysis*

In order to define dimensions of whole mobile part including the beams, the membrane and the coil, analytical equations were first considered. The relation between the membrane diameter, d, the membrane peak displacement, x_{peak}, the working frequency, f, and the acoustic power is given

TABLE II. YOUNG'S MODULUS TO DENSITY RATIO

Material	E/ρ (GPa.cm^3/gr)
C (Diamond)	1000
Al_2O_3	98
Si	71
SiO_2	49
Cr	41
Mo	32
Mo, Mn, Mg, Al, Ti, Ni, Co	24 - 27
Zn	14
Cu	12
Polyimide	2

in Eq. (2). This equation shows that the minimum working frequency defines the membrane peak displacement for a given diameter. As the new standard for high fidelity mobile audio systems stands, the target has been set for 70 dB SPL at 10 cm, and the bandwidth of 300 Hz to 20 kHz. Thickness and displacement limits defined for this microspeaker have led to 15 mm of diameter for the membrane.

$$P_{acoustic} = 0.27 d^4 f^4 x_{peak}^2 \quad (2)$$

The suspension beams disposed around the membrane are the slightly curved, but they are assimilated as straight ones for simplifying analytical modelling. As far as they are clamped to the substrate on one end and to the membrane on the other end, the maximum stress takes place at both ends. Furthermore, by taking stress and displacement relations for this kind of beam and by applying Hook's law, the following equation is formulated:

$$x = \frac{\varepsilon . l^2}{3.h} \quad (3)$$

where x is the displacement of the beam end on the membrane side, ε is the strain and l and h are respectively the beam length and thickness. Eq. (4) defines the piston mode frequency f_p of the membrane:

$$2\pi f = \sqrt{\frac{4\,E\,b\left(\frac{h}{l}\right)^3}{M_{membrane}}} \quad (4)$$

where E is the silicon Young's modulus, $M_{membrane}$ is the membrane weight and b the beam width. This piston mode frequency should be out of the microspeaker bandwidth, below the lower working frequency. Dimensions of the beams were computed using Eq. (3) and (4) with maximum strain lower than 0.1%.

After calculating beams and membrane dimensions, the coil was designed. For this purpose, the following efficiency relation was considered:

$$\eta = \frac{3.5\ \ 10^{-4}.d^4.B^2}{\rho.\rho^*} . \frac{M_{coil}}{(M_{membrane} + M_{coil})^2} \quad (5)$$

where ρ and ρ^* are respectively the coil metal density and resistivity ($\rho.\rho^*$ is $1{,}6 \times 10^{-4}$ $(kg/m^3)(\Omega.m)$ for copper), and B the radial component of the magnetic field. According to this relation, the efficiency is maximum for an equal weight of the membrane and coil. In order to maximize the radial component of the magnetic field observed by the coil, the distance between the magnets and coil should be as small as possible. That is why, ideally, the turns have to be concentrated on the edge of membrane, close to the magnets.

Calculations point out that for an assumed 0.9 T magnetic field, the efficiency is around 0.04%, which is approximately ten times more than that of conventional microspeakers.

B. Finite Element Method analysis

Once the device is sized, the structure is analyzed using FEM modelling to find out its vibration frequencies. Modal analysis of non-structured membrane reveals that at least twenty proper modes occur in the frequency bandwidth. This is known as an undesired phenomenon which deteriorates the sound quality.

The key point proposed here to overcome this problem is microstructuration of the back side of the membrane. Indeed, at the same time that membrane becomes thicker, so more rigid, holes dug in the membrane make it lighter and consequently the vibration modes will shift to higher frequencies. In this way, a ribbed structure was designed as depicted in Fig. 2-a. Every structural element such as the ribs thickness and width, the central circle radius and the number of ribs were optimized based on a trade-off between shifted vibration modes and the total weight of the membrane, which impacts the microspeaker efficiency. For the sake of modelling simplification, the weight of the coil was considered as a uniformly spread out layer on top of the membrane. Fig. 2-b shows the evolution of the drum mode frequency and the total weight as a function of the ribs number. Further analyses proves that for a membrane with 40 ribs and 83% weight reduction there are noticeably just five undesired vibration modes which intervene in the bandwidth.

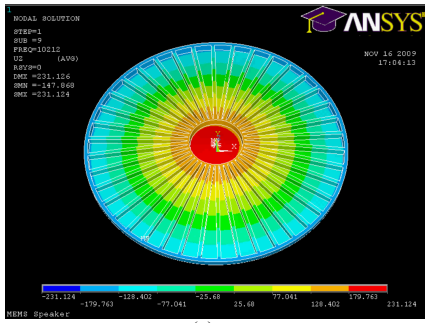

(a)

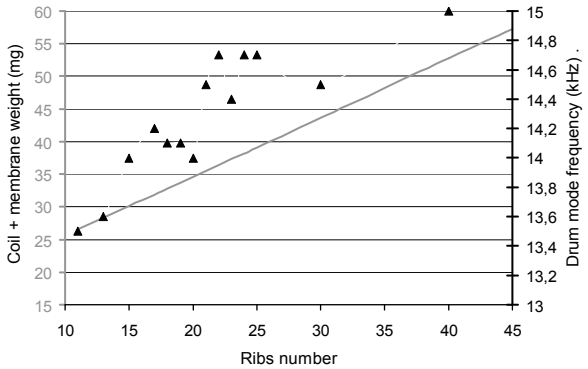

(b)

Figure 2. FEM dynamic analysis of the ribbed microstructure of the membrane (a), Drum mode frequency and total membrane weight as a function of ribs number (b).

IV. MICROFABRICATION

The device macrofabrication consists of two main parts: the microstructured membrane and the copper microcoil. The microfabrication processes of each of these main parts were optimized separately.

Forming of the silicon suspension beams and the ribbed structure of the silicon membrane is based on silicon-on-insulator (SOI) technology. Indeed, the buried silicon oxide plays a role of stop layer while etching the silicon and thus enables high thicknesses precision. Once the front side of the substrate is patterned by photolithography of Shipley S1818 resist, it is proceeded to the deep reactive ion etching (DRIE), as detailed in Fig. 3. After etching the silicon on front side (20 µm), the sample is structured on backside using Clariant AZ4562 thick resist. This resist with 10 µm thickness shows a good masking durability during 300 µm silicon DRIE. For this step of the process, the SOI substrate is temporarily bonded onto a carrier silicon substrate. To overcome the cooling problem and to accelerate heat transfer during the process, different assembly materials have been examined. Among them, Fomblin oil brings the advantages of good thermal conductivity, while enabling easy separation of the substrates after etching. Once the SOI wafer is etched on backside, the silicon oxide layer is removed from the openings using ion reactive etching (RIE). After removing the carrier wafer, the structured membranes are liberated, as depicted in Fig. 4.

Microfabrication steps of the copper coil were first optimized on silicon substrate. The steps of this process are detailed in Fig. 5. First, an insulator film of silicon oxide is deposited using Plasma Enhanced Chemical Vapour Deposition (PECVD), and then the 1 µm thick copper conductor tracks are patterned using lift-off step of TI xLift resist. To prevent short circuits among turns, the coil was not electroplated directly on top of the tracks, but on a second silicon oxide film. Two vias through this film enable electrical accesses to the inner and the outer ends of the coil. For this purpose, a silicon oxide layer of a hundred nanometres was

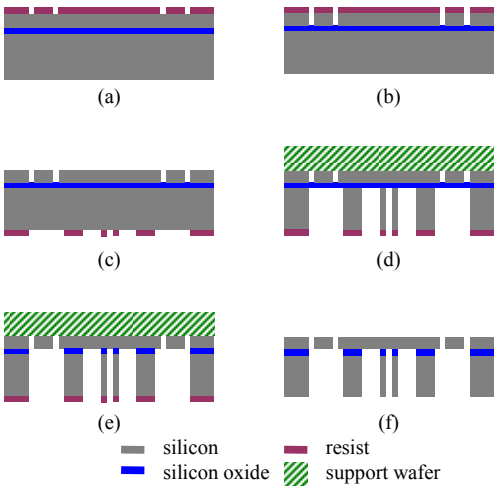

Figure 3. Membrane fabrication process, front side patterning (a), front side DRIE (b), backside patterning (c), backside DRIE (d), silicon oxide RIE (e), seperating support wafer and cleaning (f).

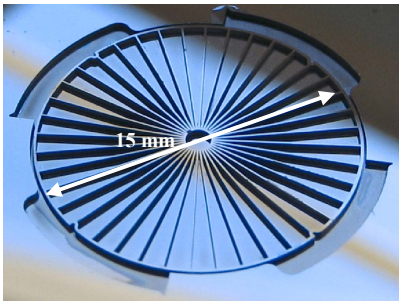

Figure 4. Structured and liberated silicon membrane (backside view).

deposited, then coated by a photoresist which was patterned in order that RIE etching opens the contact vias.

For achieving the electroplated coil, a seed layer of copper was sputtered on the silicon oxide, whose surface adhesion was ameliorated by oxygen plasma treatment. To mould the turns, a process of lithography with AZ4562 resist was developed to have 35 µm high side walls. Then the copper coil was electroplated in an electrolyze cell in which the electrolyte was agitated by a magnetic bar at 200 rpm. The most homogenous deposit was realized using -20 mA/cm^2 current density and 3 cm anode-cathode distance (Fig. 6-a). The last step consisted in removing the copper seed layer between the turns using Ion beam etching (IBE). The 35 turn copper coil realized using this process is shown in Fig. 6-b.

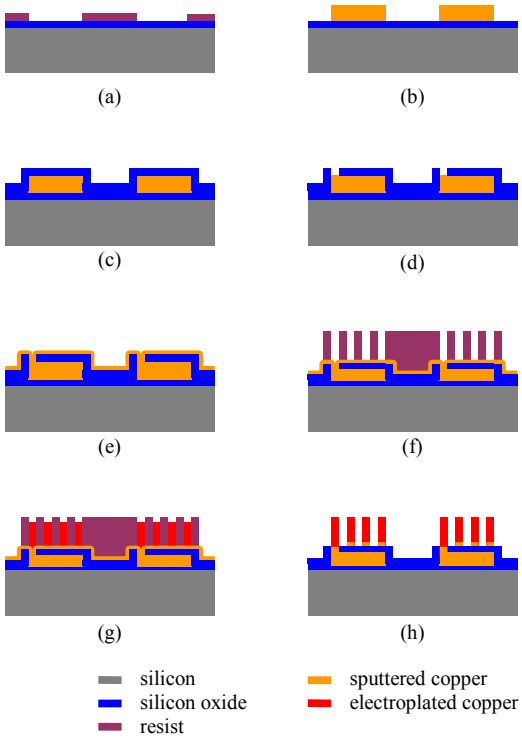

Figure 5. Coil and paths fabrication, patterning the deposited silicon oxide (a), lift-off of copper paths (b), deposit of a silicon oxide film (c), etching two vias (d), cathodic sputtering of copper seed layer (e), patterning coil (f), copper electroplating (g), seed layer etching (h)

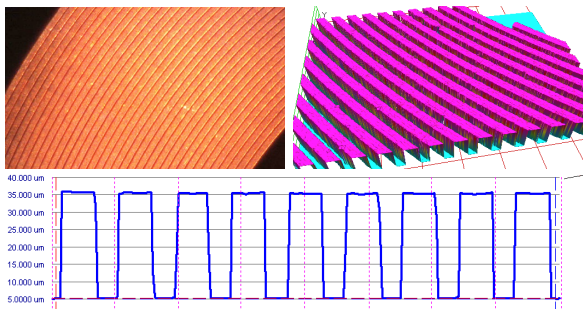

(a)

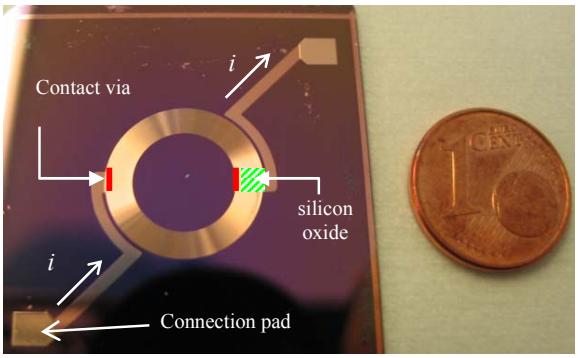

(b)

Figure 6. Quite homogeneous electroplated 30 µm copper turns, characterised by optical interferometer (a), planar copper coil on two conductor paths, separated by a silicon oxide film through which two vias pass (b)

Electrical characterization of the coil was performed using HP 4194A impedance analyzer. Resistance and inductance measurements are summarized in Table III. The resistance value correlates with that of theoretical calculations. However, simulations for inductance showed that the inductance value may considerably change, depending on the thickness of the insulation layer between the coil and the substrate, and depending also on the substrate resistivity. These simulations show that the inductance may be increased with thicker insulator layer between the coil and the silicon substrate.

V. CONCLUSION AND FUTURE WORK

Novel electrodynamic MEMS microspeaker design was presented in this paper. Originality of the structure lies in the use of silicon microstructured membrane, whose very important stiffness favours high fidelity sound reproduction and whose lightness is a key factor for efficiency.

TABLE III. ELECTROPLATED COPPER COIL ELECTRICAL CHARACTERISTICS

Frequency	Resistance	Inductance
1 kHz	11 Ω	12 µH
10 kHz	11 Ω	12 µH
30 kHz	11.9 Ω	10 µH
100 kHz	13 Ω	7.2 µH

Design, modelling and simulation results of the membrane and its suspension beams were presented. The microfabrication process based on SOI technology enabled to fabricate light and stiff membranes, with high thickness precision of the micromachined layers. This point is peculiarly important regarding the suspension beams and the dynamic balance of the whole mobile structure. Separately, a planar copper coil, quite uniform in thickness, was electroplated on top of two sputtered copper tracks used as inner and outer electrical connexions.

Ongoing work focuses on mechanical dynamic characterization of the membrane and the suspension beams. Technological processes developed for microfabrication of the silicon suspended membrane and the copper coil will be then combined to realize the final device. Assembly of the magnets will enable the last characterization step, which will consist in determining experimentally the electrical, mechanical and acoustical characteristics of the micro speaker.

ACKNOWLEDGMENT

This work has been financially supported by the French Agence Nationale pour la Recherche. The authors would like to thank the staff of the University Technological Center CTU IEF-MINERVE for their help and technical support.

REFERENCES

[1] S. Je et al., “A compact and low-cost MEMS loudspeaker for digital hearing aids,” IEEE Transactions on Biomedical Circuits and Systems, 2009, Vol. 3, No. 5, pp. 348-358.

[2] S. H. Yi and E. S. Kim, “Micromachined piezoelectric microspeaker,” Japanese Journal of Applied Physics, 2005, Vol. 44, No. 6A, pp. 3836–3841.

[3] H. C. Cho, S. C.Ur, M. S. Yoon, and S. H. Yi, “Dependence of material properties on piezoelectric microspeakers with AlN thin film, ” Proceedings of the 3rd IEEE Int. Conf. on Nano/Micro Engineered and Molecular Systems January 6-9, 2008.

[4] S. C. Ko, Y. C. Kim, S. S. Lee, S. H. Choi, S. R. Kim, “Micromachined piezoelectric membrane acoustic device,” Sensors and Actuators, 2003, A 103, pp. 130–134.

[5] S. S. Lee and R. M. White, “Piezoelectric cantilever voltage-to-frequency converter,” Sensors and Actuators, 1998, A 71, pp. 153-157.

[6] P. Rangsten, L. Smith, L. Rosengren, and B. Hok, “Electrostatically excited diaphragm driven as a loudspeaker,” Sensors and Actuators, 1996, A 52, pp. 211-215.

[7] R. C. Roberts, J. Du, A. O. Ong, D. Li, C. A. Zorman, and N. C. Tien, “Electrostatically driven touch-mode poly-SiC microspeaker,” IEEE Sensors 2007 Conference.

[8] R. Heydt, R. Kornbluh, R. Pelrine, and V. Mason, “Design and performance of an electrostrictive-polymer-film acoustic actuator,” Journal of Sound and Vibration, 1998, 215(2), pp. 297-311.

[9] L. Xiao et al., “Flexible, stretchable, transparent carbon nanotube thin film loudspeakers,” Nano Letters, 2008, Vol. 8, No. 12, pp. 4539-4545.

[10] M. C. Cheng, W. S. Huang, and S. R. S. Huang, “A silicon microspeaker for hearing instruments,” Journal of Micromechanics and Microengineering, 2004, Vol. 14, pp. 859–866.